SMAR 2017 – Fourth Conference on Smart Monitoring,
Assessment and Rehabilitation of Civil Structures

SMAR 2017

Fatigue and durability of laminated carbon fibre reinforced polymer straps for bridge suspenders

Giovanni Pietro Terrasi[1], Fabio Baschnagel[1], Jing Gao[2], Robert Widmann[3], Urs Meier[4]

[1] Mechanical Systems Engineering Lab, Empa, Dübendorf, Switzerland
[2] Department of Civil Engineering, University of Xiamen, Xiamen, PRC
[3] Structural Engineering Lab, Empa, Dübendorf, Switzerland
[4] Director emeritus, Empa, Dübendorf, Switzerland

ABSTRACT: This paper focuses on the fretting fatigue behaviour of novel pin-loaded carbon fibre reinforced polymer (CFRP) straps studied as models for corrosion resistant suspenders of half-through arch bridges. Two types of straps were tested: small model straps and large full-scale straps. In a first phase, eight fully laminated pin-loaded CFRP model straps were subjected to an ultimate tensile strength test. Thereafter, and in order to assess the durability, 26 model straps were subjected to a fretting fatigue test, in which ten did not fail. A S-N curve was generated for a load ratio of 0.1 and a frequency of 10 Hz, showing a fatigue limit of the straps around the epoxy matrix fatigue limit strain, corresponding to 46% of the model straps' ultimate tensile strength (σ_{UTS}). The fatigue limit was defined as 3 million load cycles ($N = 3\times10^6$), but tests were even conducted up to $N = 11\times10^6$. In a second phase, one full-scale strap was tested for its ultimate tensile strength and two full-scale straps were fatigue tested. The influence of the fatigue testing on the straps' residual mechanical properties was also assessed for both strap types. Catastrophic failure of all straps was initiated in their vertex areas.

1 INTRODUCTION

By weighing six times less than comparable steel tension members, CFRP tension members are of growing importance in the sailing and construction industry, Composites World (2015), where they are starting to replace steel members that are prone to environmental influences such as salt water, which can cause stress corrosion. However, CFRPs are affected by certain environmental influences like UV radiation (epoxy matrix) and in applications such as suspenders used for half-through arch bridges, dynamic fatigue is highly relevant, Gao et al (2013). In the present study, the fretting of the contacting surfaces further increases the material degradation, as reported by Friedrich et al (1987) and Schulte et al (1987, 1988). Compared to isotropic materials such as metals, ceramics or polymers, the damage modes and crack propagation are much more complex in CFRPs and depend on a variety of factors. Nevertheless, Reifsnider (1981) characterized the fatigue behaviour of multiaxial fibre reinforced composites (FRPs) in a general way and divided it into three stages. In the first stage, the damage develops at a very rapid rate within the first 10%–15% of the laminate's life. In this stage, the major damage mode is matrix cracking in the laminae with the most off-axis fibre orientation. This intralaminar matrix cracking between the fibres reaches uniform saturation spacing at the end of stage I, called characteristic damage state (CDS). In stage II, comprising 70%–80% of the fatigue life, damage is still initiated and the already existing damages continue to grow, but at a

much slower rate, until the laminate is severely damaged and then enters stage III, where the damage process is accelerated again until final failure of the laminate.
For purely unidirectional (UD) CFRP laminates, the situation is different, since no off-axis plies are present. However, since carbon fibres show excellent fatigue behaviour, Morgan (2005), the matrix and its interaction with the fibres remains the limiting factor in the composite's fatigue life, Curtis (1982, 1986, 1987). Based on this idea, Talreja (1981) introduced a fatigue life diagram in which he suggests that the fatigue life of a unidirectionally reinforced polymer is governed by the composite's quasi-static fracture strain and the matrix fatigue limit strain. Given the fibres insensitiveness to fatigue and neglecting possible fretting, the diagram states that no damage progression takes place in the composite below the epoxy matrix fatigue limit strain of $\varepsilon_{mf} = 0.6\%$, Dharan (1975).
In the presence of fretting, Friedrich et al (1987) and Schulte et al (1987, 1988), could show how an increased normal contact force leads to a more pronounced decrease in fatigue strength and that the influence of the contact force increases if the contacting ply is oriented in the primary loading direction. This is also the case in the examined CFRP straps, and the goal of this study was to investigate the fretting fatigue behaviour of these straps in order to improve the durability of existing CFRP tension members. In addition to the model test, full scale test on comparable tension members were performed.

2 MATERIALS AND MANUFACTURING

The materials used for the production of the out of autoclave (OOA) carbon fibre/epoxy (CF-EP) prepreg were a XB3515/Aradur® 5021 matrix system by Huntsman (Huntsman Advanced Materials GmbH, Basel, Switzerland) and intermediate modulus IMS60 carbon fibres by Toho Tenax® (Toho Tenax Europe GmbH, Wuppertal, Germany) with a reported Young's modulus of 290 GPa and tensile strength of 5600 MPa. The prepreg tapes with nominal widths of 9, 12 and 48 mm were produced by Carbo-Link AG in Fehraltorf, Switzerland and reported to have a V_f of 62% ± 2%. The laminate's average experimental tensile strength was 2567 ± 58 MPa with a longitudinal (fibre parallel) elastic modulus E_{11} of 168 ± 6.6 GPa and an average ultimate tensile strain ε_{11u} of 1.52% ± 0.23%. Investigations on the laminate quality of the hand laminated model straps revealed an average V_f of 66% and a void content of less than 1%. The pultruded T300 CF-EP pins used for the loading of the model straps had a V_f of 60–65%. The model CFRP straps had a thickness t of 1 mm, a shaft length L of 250 mm, a width w of 12 mm or 9.7 mm, depending on the prepreg tape used, and an inner radius r of 10 mm. The full scale straps were manufactured from the 48 mm wide tape by winding it around two 50 mm wide titanium connector eyes (r_i = 90mm, r_o = 180 mm) to a final thickness of 10 mm. The three straps (Strap I-III) had a length of 3012 mm, 3015 mm and 3017 mm and a free-length circular cross-sectional area of 871 mm^2, 860 mm^2 and 845 mm^2, respectively.

3 EXPERIMENTAL SETUP

3.1 Model Straps

The ultimate tensile strength (σ_{UTS}) and fretting fatigue tests on the model straps were conducted on a servo-hydraulic test machine (type 1251, Instron®, Norwood, MA, USA). The tensile strength tests were performed under displacement-control at a cross-head speed of 2 mm/min. The corresponding fatigue tests were performed under load-control at a frequency f of 10 Hz and a load ratio R of 0.1. Figure 1 illustrates the test setup of a model strap and pin in the testing machine. The pultruded CFRP pin is placed in a fork-like steel adapter that is screwed to the

cross-head of the testing machine. The picture also shows the type K thermocouple that was glued to the outside of the straps in order to monitor the temperature development in the critical (vertex) area. This was felt to be an important aspect to assess since temperature increases, e.g. from hysteretic heating at high test frequencies or due to fretting, can reduce the dynamic performance of a composite structure. Whenever narrow straps were tested, thin copper washers were placed on both sides of the strap to ensure the lateral support of the strap, which is reported to reduce stress concentrations, Schürmann (2007).

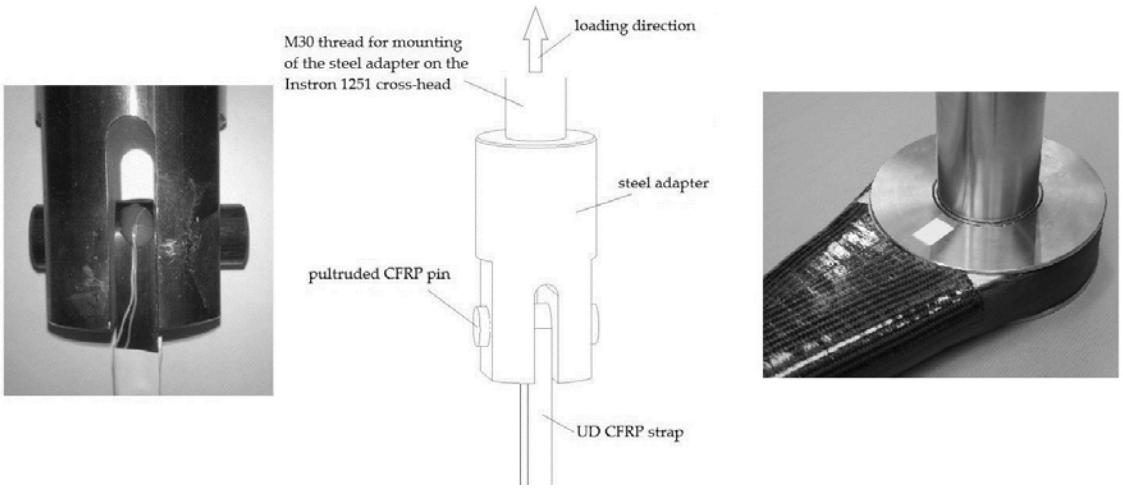

Figure 1. Test setup for model straps (left) and picture of a full-scale strap before testing (right).

3.2 Full-Scale Straps

The full-scale straps were tested on an in-house test machine containing an Amsler P960 pulsator. The titanium connectors of the full-scale straps were mounted on a metal bolt with an intermediate plain bearing bush, see Figure 1. The quasi-static tensile strength test of Strap III was performed under force-control at 90 kN/min. Strap I was fatigue tested at a frequency of 4.2 Hz and R = 0.2 for 0.8×10^6 load cycles and additional 11.6×10^6 load cycles at a load ratio of 0.42. The corresponding upper stress levels (σ_u) were 660 MPa and 530 MPa, respectively. Strap II was fatigue tested at a load ratio of 0.42 and a frequency f of 4.2 Hz for 11.3×10^6 load cycles at an upper stress level σ_u of 537 MPa.

4 EXPERIMENTAL RESULTS AND DISCUSSION

4.1 Quasi-Static Behaviour

Prior to the fretting fatigue tests, thirteen model straps and one full-scale strap were tested for their ultimate tensile strength. The results of the quasi-static tensile tests performed on the eight wide (12 mm) and five narrow (9.7 mm) model straps and full-scale Strap III are given in Table 1. Two different types of model straps were tested since the 12 mm wide straps required a lateral machining of the straps in order to fit into the adapter. The 9.7 mm model straps, on the contrary, did not require this kind of invasive post-processing which was suspected to negatively influence the mechanical performance of the straps. However, Baschnagel et al (2016) only found a lower standard deviation (SD) of the mechanical properties for the non-machined straps but no significant influence on their average values. The low tensile strength of

the model straps were explained with stress concentrations of up to 1.3 in their vertex areas and the presence of wavy fibres.

Table 1. Average quasi-static tensile strength and stiffness of pristine wide (12 mm) and narrow (9.7 mm) model straps and quasi-static tensile strength of full-scale Strap III. The fibre parallel elastic modulus E_{11} (GPa) of the model straps was measured with strain gauges (E_{11_SG}) and a linear encoder (E_{11_LE}). The corresponding composite strains at failure ε_{cf} (%) were measured with the strain gauges.

Strap	$\sigma_{UTS,P}$ (MPa)	E_{11_SG} (GPa)	E_{11_LE} (GPa)	ε_{cf} (%)
wide	1'624±121	177.8±8.6	175.8±12.1	0.99±0.04
narrow	1'714±55	174.4±1.1	166.2±6.2	1.00±0.05
full-scale	2'124	-	-	-

4.2 Fretting Fatigue

4.2.1 S-N Curve

Figure 2 shows the S–N curve obtained from the fretting fatigue testing of 12 mm wide pin-loaded model straps (circular markers). A strap was defined to have reached the fatigue limit once it endured more than 3 million load cycles. In order to confirm this, one model strap was tested for 11.089 $\times 10^6$ load cycles at the fatigue limit stress (750 MPa) without failure. The two full-scale straps were also tested for over 11×10^6 load cycles but at a different load ratio (see section 3.2). For the sake of completeness, the full-scale strap tests are also given in Figure 2 (square markers). Markers containing a cross indicate failed straps.

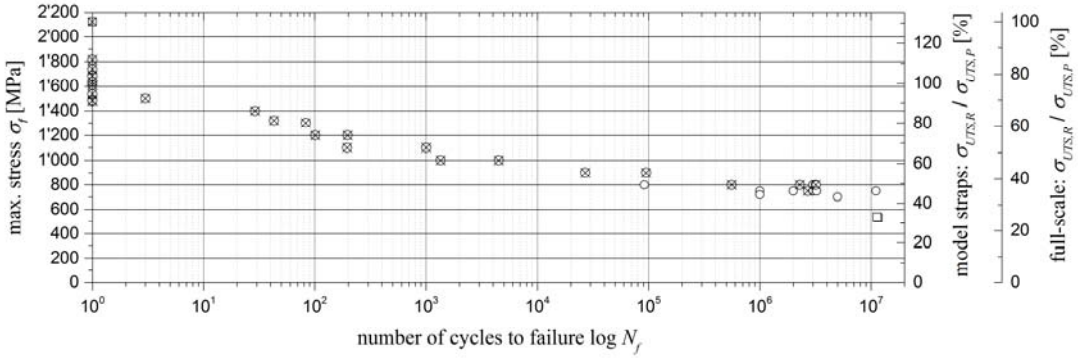

Figure 2. S-N curve of the 12 mm wide model straps (circular markers), listing the upper stress level (σ_u) as a function of endured load cycles at failure (N_f). The results of the full-scale strap tests (at a different R) are also given (square markers).

4.2.2 Residual Properties

The residual mechanical properties of straps tested without failure after 1, 2, 3 and 11 million load cycles were tested in quasi-static tensile tests until failure. The test setup was the same as for the pristine straps. Table 2 lists the results of these measurements.

Table 2. Average residual strength ($\sigma_{UTS,R}$) and stiffness properties of wide model straps after 1, 2, 3 and 11 million load cycles at an upper stress level (σ_u) of 720–750 MPa and residual strength of full-scale straps after 11 million load cycles at σ_u = 530-537 MPa. The fibre parallel elastic modulus E_{11} of the model straps was calculated from linear encoder measurements (E_{11_LE}).

Strap	$\sigma_{UTS,R}$ (MPa)	E_{11_LE} (GPa)	$\sigma_{UTS,R}/\ \sigma_{UTS,P}$ (%)
wide	1'620±65	165.9±4.0	99.8
full-scale	1'491± 79	-	70.2

Comparing the residual stiffness's of the model straps tested for $N \geq 1\times10^6$ to the stiffness of an average pristine strap reveals a slight stiffness reduction over time of up to 10%. The ultimate tensile strength of the model straps on the other hand is hardly affected by the fretting fatigue loading. Furthermore, the standard deviation (SD) is much lower in the fatigue tested model straps and first signs of (further) damage occured only after the straps have reached approximately 80% of their ultimate tensile strength. In pristine model straps, first signs of damage were observed just above 50% of their ultimate tensile strength. Due to the low number of test specimens and the slightly varying testing parameters, the residual strength measurements of the full-scale straps show a higher SD. They also suffer from a more pronounced strength decrease which could be related to the harder connector material in combination with a larger contacting surface.

4.2.3 Damage Modes

The damage modes of all fretting fatigue tested model straps were similar. First, visible damage always occurred in the form of delamination of the inner- and outermost layers in the shaft with the overlapping plies. The delaminations started at the free ends of the tape and propagated along the shaft until they stopped in the vertex area. Another damage mode was longitudinal matrix cracking. This damage mode occurred solely in the inner- and outermost plies and did not propagate over the vertex areas of the model straps either. However, none of the above failure mechanisms could be directly attributed to a certain stress level during testing. The failure of all straps was initiated in the vertex areas and led to fibre bursting in one or both shafts. Failure of the full-scale Strap III occurred in a similar way, whilst the fatigue tested full-scale straps showed no signs of fibre bursting in the shaft but rather fibre parallel matrix cracking.

4.2.4 Fretting Behaviour

The fretting behaviour of the contacting surfaces was investigated differently for the two types of straps. By placing a transparent adhesive tape on the model strap and CFRP pin surfaces just after testing, the fretting products of these tests could be investigated. The tapes were placed on a sheet of paper and investigated under an optical microscope (ZEISS Axioplan in reflected-light mode). Figure 3 shows two representative pictures of a strap and a pin. Clearly visible are the carbon fibre particle accumulations just outside the vertex area of the strap. In accordance with Schulte et al (1987) and Cirino et al (1988(1), 1988(2)), the main damage mode observed on the strap (sliding of the contacting surface in fibre direction) was fibre thinning, resulting in small carbon particles. The fretting products on the pin on the other hand consist mostly of short, broken and pulled-out carbon fibres with parts of neat resin still attached to the fibres. This is also reported by Cirino et al (1988(1), 1988(2)), Sung et al (1979), Winistörfer (1999) and Schön (2004) to be typical for sliding perpendicular to the fibres. Clear signs of a

homogeneous graphite particle film covering the contact area that might act as a lubricant were not detected. However, the graphite particle aggregations just outside the vertex areas of the strap suggest a particle transport from the fretting areas to the free surfaces of the shaft. This would require that the particles do build, at some point, an intermediate film between the pin and the strap which would contribute to a reduction of the coefficient of friction.

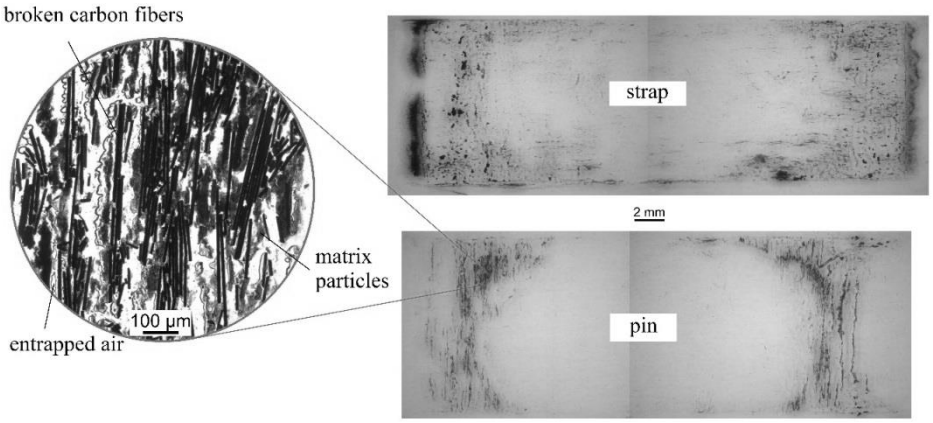

Figure 3. Fretting products of a model strap after 3×10^4 load cycles (top) and a pin after $N = 10^6$ (bottom). Both images show fretting products from tests conducted at a load level of 720 MPa.

The contacting surfaces of the full-scale straps were investigated under a scanning electron microscope (SEM, FEI ESEM XL30). Figure 4 shows three pictures of typical surface conditions after testing. Figure 4c shows the surface of Strap III in contact with the titanium connecter eye in the vertex area. As the strap was not exposed to fatigue testing, the fibres (dark) are still well embedded in the intact matrix (light) and show no signs of fibre thinning. In the regions close to the top (crown) where the relative movement between strap and connecter eye is relatively small, the surface of the fatigue tested Strap I was similar. Further away from the top (crown) of the strap, see Figure 4b, the fibres are still intact, but the matrix suffered from the small relative movement between the strap and the connecter eye. This matrix deterioration is even more pronounced in the vertex areas of fatigue tested straps, Figure 4a, where the fibres are not visibly embedded in the matrix anymore. The fibre parallel fretting also caused fibre thinning (Figure 4a, left) and the fretting products agglomerate and cover the fibres (Figure 4a, right). These particle agglomerations consist of compressed fretting products with particle diameters of 30-100 nm.

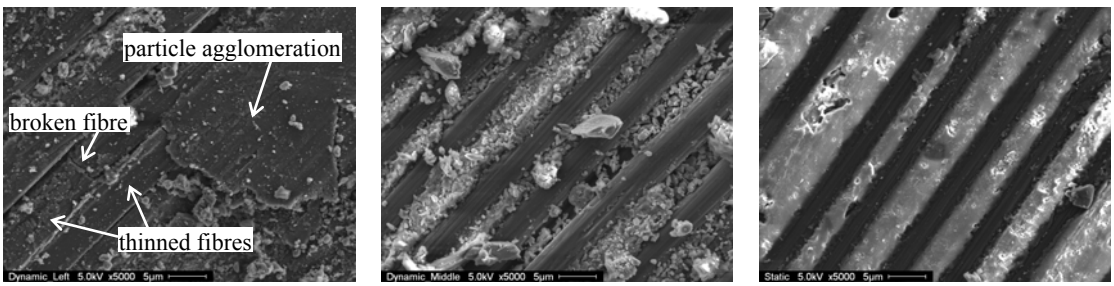

a) b) c)

Figure 4. Typical SEM pictures of the full-scale strap surfaces in contact with the titanium connecter eye. The pictures were taken in the vertex area of Strap I, Figure 4a, close to the top (crown) area of Strap I, Figure 4b, and in the vertex area of Strap III, Figure 4c, after failure of the straps.

4.2.5 Temperature

Due to the high testing frequencies, the temperature on the outside of the straps was monitored during all fatigue tests. The thermocouples on the outside of the model straps measured a significant initial temperature increase with a peak within the first 10^4 load cycles for all straps. After this peak, the temperature decreases and levels out before increasing again prior to failure of the strap. As the initial peaks never exceeded 65 °C, which is far below the glass transition temperature (T_g = 140 °C) of the CFRP, and the considered laminate is thin, these temperature increases can be considered non-critical. The temperature measurements on the outside of the full-scale Strap I revealed a maximum temperature of 80 °C after 2×10^4 load cycles. As the temperature did not decrease within the subsequent 5000 load cycles and with a laminate thickness of 10 mm, it had to be assumed that the temperature inside the laminate was much higher. Hence, the test was paused and the testing parameters were adjusted (see section 3.2). After these adjustments, the temperature didn't exceed 50 °C, which was also the maximum temperature measured on Strap II.

5 CONCLUSIONS

The fretting fatigue behaviour of pin-loaded CFRP straps under tensile loading was presented in this study. The investigated straps had been subjected to ultimate tensile strength and fretting fatigue tests up to 11×10^6 load cycles. A total number of 28 straps, 26 wide model straps (12 mm) and two full-scale straps, were subjected to fretting fatigue loading. The results were used to generate an S–N curve. The following conclusions can be drawn on the basis of the study described in this paper:

- The pin-loaded model CFRP straps showed a fatigue limit stress of 750 MPa, which corresponds to 46% of their ultimate tensile strength. The fatigue limit was defined to be reached once a strap endured more than 3×10^6 load cycles, and one model strap was tested without failure for 11.09×10^6 load cycles to confirm this.
- The experimentally determined fatigue limit of the model straps corresponds to the matrix fatigue limit strain of 0.6%, which is reported by Talreja (1981) to be the ultimate lower bound for a UD fibre reinforced composite fatigue limit.
- Clear signs of a graphite film acting as lubricant between pin and strap were not found. However, the carbon fibre particle accumulations just outside the vertex area of the inner strap surface require a transport of these particles from the fretting areas to the outside. This in turn means that a particle film is present at some point and contributes to a reduction of the coefficient of friction.
- The pristine full-scale strap showed a significantly higher ultimate tensile strength than the model straps. This might be attributed to the connector eye with an improved geometry, mitigating the stress concentrations in the vertex areas.
- The two full-scale straps were fatigue tested below the matrix fatigue limit strain and did not fail ($N \geq 11\times10^6$). This corroborates the above findings for the model straps.
- The fretting of the straps on their respective connector leads to a decrease in residual tensile strength. This effect was more pronounced in the full-scale straps. A possible reason might be the harder connector material and larger contact area, leading to a stronger material deterioration in the CFRP strap.

- Although the fretting behaviour of the presented straps needs to be investigated further, it could be shown that CFRP tension members can compete with the well-established steel tension members.

ACKNOWLEDGMENTS

The authors would like to thank the whole Mechanical Systems Engineering Laboratory of Empa Dübendorf. Special thanks go to Andreas Brunner, Christian Affolter and Daniel Völki. Further thanks go to Christian Loosli, Gerald Kress and Paolo Ermanni from the Laboratory of Composite Materials and Adaptive Structures at ETH Zürich.

REFERENCES

Baschnagel, F, Rohr, V, Terrasi, GP. 2016 Fretting Fatigue Behaviour of Pin-Loaded Thermoset Carbon-Fibre-Reinforced Polymer (CFRP) Straps. *Polymers*, 8(4), 124.

Cirino, M, K. Friedrich, R.B. Pipes. The Effect of Fiber Orientation on the Abrasive Wear Behavior of Polymer Composite Materials. *Wear*, 121:127-141, 1988(1).

Cirino, M, K. Friedrich, R.R. Pipes. Evaluation of polymer composites for sliding and abrasive wear applications. *Composites* 19-5:383-392, 1988(2).

CompositesWorld, March 2015. 2015. Gardner Business Media Inc.. Available online: http://cw.epubxp.com/i/467593-mar-2015 (accessed on April 1 2016)

Curtis, P.T. *RAE Technical Report TR82031;* RAE (now DRA), Farnborough, UK, 1982.

Curtis, P.T. An investigation of the mechanical properties of improved carbon fibre materials. *RAE Technical Report TR86021,* RAE (now DRA), Farnborough, UK, 1986.

Curtis, P.T. A review of the fatigue of composite materials. *RAE Technical Report TR87031,* RAE (now DRA), Farnborough, UK, 1987.

Dharan, C.K.H. Fatigue Failure Mechanisms in a Unidirectionally Reinforced Composite Material. *Fatigue in Composite Materials, ASTM STP,* 569:171-188, 1975.

Friedrich, K, S. Kutter, K. Schulte. Fretting Fatigue Studies on Carbon Fibre/Epoxy Resin Laminates: I-Design of a Fretting Fatigue Test Apparatus. *Compos. Sci. Technol.,* 30:19-34, 1987.

Gao, J, C.M. Chen, A. Winistörfer, U. Meier. Proposal for the application of carbon fiber reinforced polymers (CFRP) for suspenders of arch bridges in China. *Proceedings of SMAR 2013 the 2nd Conference on Smart Monitoring, Assessment and Rehabilitation of Civil Structures, Istanbul, Turkey,* September 9-11 2013.

Morgan, P. *Carbon fibers and their composites.* CRC Press Taylor & Francis Group, 2005.

Reifsnider, KL, AL Highsmith. Characteristic damage states: A new approach to representing fatigue damage in composite materials. *Materials, Experimentation and Design in Fatigue.* F. Sherrat, J.B. Sturgeon, Eds. Westbury House: Guildford, UK, 1981.

Schön, J. Coefficient of friction for aluminum in contact with a carbon fiber epoxy composite. *Tribol. Int.,* 37-5:395-404, 2004.

Schulte, K, K. Friedrich, S. Kutter. Fretting Fatigue Studies on Carobn Fibre/Epoxy Resin Laminates. Part II: Effects of a Fretting Component on Fatigue Life. *Compos. Sci. Technol.,* 30:203-219, 1987.

Schulte, K, K. Friedrich, S. Kutter. Fretting Fatigue Studies on Carbon Fibre/Epoxy Resin Laminates: III-Microscopy of Fretting Fatigue Failure Mechanisms. *Comp. Sci. Technol.,* 33:155-176, 1988.

Schürmann, H. *Konstruieren mit Faser-Kunststoff-Verbunden,* Springer, 2007.

Sung, N-H, N.P. Suh. Effect of Fiber Orientation on Friction and Wear of Fiber Reinforced Polymeric Composites. *Wear* 53:129-141, 1979.

Talreja, R. Fatigue of composite materials: damage mechanisms and fatigue-life diagrams. *Proc. R. Soc. Lond. A.,* 378:461-475, 1981.

Winistörfer, A. *Development of non-laminated advanced composite straps for civil engineering applications.* Diss. University of Warwick, 1999.